Resonant Hopf triads in a delayed optical pattern-forming system

Yu. A. Logvin and N. A. Loiko
Institute of Physics, Belarus Academy of Sciences, 70 F. Skaryna Avenue, Minsk 220072, Belarus
(Received 27 March 1997)

It is demonstrated that the Hopf spatiotemporal modes can build stable resonant triads in an optical pattern-forming system with delay. The resonant Hopf triads correspond to dissipative structures in the form of drifting patterns of rhombic, hexagonal, or rhomboidal symmetry. Multistability of different patterns is found in numerical simulations. [S1063-651X(97)00809-X]

PACS number(s): 82.40.Ck, 05.70.Fh, 42.65.Sf, 47.54.+r

I. INTRODUCTION

Resonant interaction of waves is actively studied in different branches of nonlinear physics. If quadratic nonlinearity dominates, effective exchange of energy between the modes composing a resonant triad occurs under conditions

$$\Omega_1 \pm \Omega_2 \pm \Omega_3 = 0, \tag{1}$$

$$\mathbf{k}_1 \pm \mathbf{k}_2 \pm \mathbf{k}_3 = \mathbf{0}, \tag{2}$$

where Ω_i and $\mathbf{k}_i$ $(i=1,2,3)$ are frequencies and wave vectors of resonant modes, respectively. Examples of such resonant triad interaction are well known in plasma physics [1,2], hydrodynamics [3,4], physics of ferromagnets [5,6], and nonlinear optics [7].

In dissipative systems demonstrating spontaneous pattern formation [8], triadic mode interaction is manifested, first of all, in formation of static hexagonal structures with all frequencies Ω_i being zero and the wave vectors $\mathbf{k}_i$ forming an equilateral triangle. Recently, resonant interaction of one static $(\Omega_1=0)$ and two Hopf $(\Omega_2=-\Omega_3)$ modes has been discussed in the context of one-dimensional (1D) Turing structures [9] and two-dimensional (2D) patterns in a nonlinear optical system [10]. Subharmonic instability of a Hopf mode has also been considered in the 1D Brusselator model [11].

Here, we continue our previous studies [10,12] of optical patterns in a single-feedback-mirror system where delay effects are taken into consideration. In this paper we show that Hopf modes belonging to different families (i.e., differing by Ω_i and/or $\mathbf{k}_i$) may form stable triadic construction. Depending on the relations between the lengths of the vectors $\mathbf{k}_i$, emergence of drifting patterns of hexagonal, rhombic, or rhomboidal symmetry may occur. Frequencies Ω_i determine the velocity of the drift. Moreover, our numerical simulations show that multistability of different triadic Hopf patterns is possible.

Triadic Hopf patterns become possible in our system due to interplay between the effects of diffraction and delay owing to light propagation in the feedback loop. It is well known that in a nonlinear system with delay, oscillating regimes with the frequencies equal to $2\pi/2\tau$ (where τ is a delay time) and its multiples are possible [13–15]. Thus the time delay causes Hopf instability in our system. In its turn, diffraction spreading of light, in combination with nonlinear mechanisms of light-matter interaction, governs simultaneous excitations of several families of modes (multiconical emission) [16–19]. The spatial characteristics of these modes are determined by the Talbot effect well known in optics [20]. As a result, developing Hopf modes form resonant triads which satisfy the conditions of phase matching in space and in time.

Below, after description of the model, we present results of a linear stability analysis and, further, examples of the triadic Hopf patterns obtained in numerical simulations.

II. MODEL DESCRIPTION

The single-feedback-mirror system in different modifications has become very popular in studies of optical pattern formation during the last few years [16–19,10]. Its principal scheme is presented in Fig. 1. A plane wave light field with amplitude e_0 is incident on a thin layer of nonlinear material. After transmission through the layer, light is fed back by a

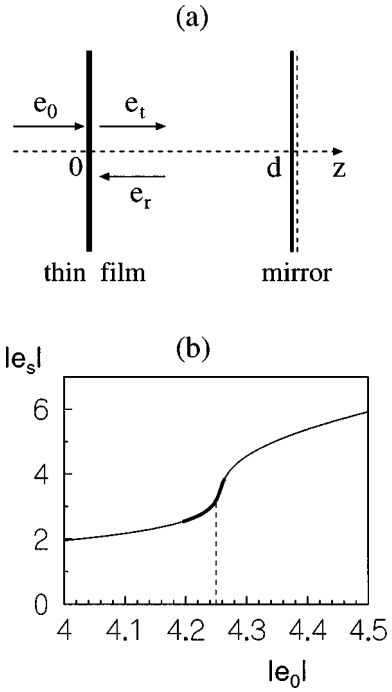

FIG. 1. (a) Single-feedback-mirror optical scheme. See text. (b) Steady state characteristic determined by Eq. (9) at $C=3.5$ and $\delta=-2$. The interval of instability is marked by the solid line.

mirror which is set parallel to the layer in distance d. Coupling between the transmitted field (amplitude e_t) and the reflected (amplitude e_r) is given by the diffractional paraxial operator $\hat{F}$:

$$e_r(\mathbf{r}_\perp,t)=\hat{F}e_t(\mathbf{r}_\perp,t-\tau)\equiv e^{-i(d/k)\Delta_\perp}e_t(\mathbf{r}_\perp,t-\tau), \quad (3)$$

where k is the light wave number, and $\Delta_\perp$ is the Laplacian over transverse coordinates $\mathbf{r}_\perp=\{x,y\}$. It is supposed that the mirror reflectivity is equal to unity, and the distance d contains an integer number of light half wavelengths.

We assume that a film of two-level centers has a thickness much less than the wavelength of incident light. This allows us to neglect diffraction and delay during light propagation inside the film. In this case, the transmitted and external incident fields are related as [21]

$$e_t(\mathbf{r}_\perp,t)=e_0-i2Cr(\mathbf{r}_\perp,t), \quad (4)$$

where $r(\mathbf{r}_\perp,t)$ is the normalized polarization emitted by the two-level centers in the film, and the constant C is the bistability parameter [22].

Interaction of light with two-level centers is described by the optical Bloch equations [23]

$$\dot{r}=(-1+i\delta)r+iew, \quad (5)$$

$$\dot{w}=-\gamma(w+1)+\gamma i(e^*r-r^*e)/2, \quad (6)$$

where w is the population difference, δ is the frequency detuning between the incident field and two-level transition, and $\gamma=T_2/T_1$ is the ratio between the longitudinal and transversal relaxation times. The expression for the field e driving the centers in the film is given by

$$e(\mathbf{r}_\perp,t)=e_0+e_r(\mathbf{r}_\perp,t)-i2Cr(\mathbf{r}_\perp,t). \quad (7)$$

It is seen that the total field in the film consists of two fields illuminating the layer from both sides, as well as of the superradiance field proportional to the polarization r.

III. STEADY STATE AND STABILITY

The homogeneous steady state solution is given by the following expressions for population difference and polarization:

$$w_s=-\frac{1+\delta^2}{1+\delta^2+|e_s|^2}, \quad r_s=\frac{(\delta-i)e_s}{1+\delta^2+|e_s|^2}, \quad (8)$$

with the nonlinear algebraic equation for the steady state magnitude of the field e_s inside the film:

$$|e_0|^2=|e_s|^2\left[\left(1+\frac{4C}{1+\delta^2+|e_s|^2}\right)^2+\left(\frac{4C\delta}{1+\delta^2+|e_s|^2}\right)^2\right]. \quad (9)$$

The characteristic presented in Fig. 1(b) shows dependence $e_s(e_0)$ for $C=3.5$ and $\delta=-2$. If we increase parameter C (or decrease $|\delta|$), the characteristic becomes bistable [22,24].

Analyzing stability of the steady state with respect to perturbations $\delta w,\delta r\propto\exp(\lambda t+i\mathbf{k}_\perp\mathbf{r}_\perp)$ we obtain the eigenvalue problem:

$$\begin{pmatrix} \Delta+2Cw_s(1+e^{i\theta-\lambda\tau}) & 0 & 2ie_0+4Cr_s \\ 0 & \Delta^*+2Cw_s(1+e^{-i\theta-\lambda^*\tau}) & -2ie_0+4Cr_s^* \\ i\gamma e_0-\gamma Cr_s^*(3+e^{i\theta-\lambda\tau}) & -i\gamma e_0-\gamma Cr_s(3+e^{-i\theta-\lambda^*\tau}) & -\gamma \end{pmatrix}\begin{pmatrix}\delta r\\ \delta r^*\\ \delta w\end{pmatrix}=\lambda\begin{pmatrix}\delta r\\ \delta r^*\\ \delta w\end{pmatrix}, \quad (10)$$

where $\Delta=-1+i\delta$ and $\theta=k_\perp^2 d/k$ is a diffractional parameter whose origin is evident due to the form of the diffractional operator $\hat{F}$ [see Eq. (1)].

Thick partition of the steady state characteristic in Fig. 1(b) corresponds to the static instability ($\mathrm{Re}(\lambda)=0,\mathrm{Im}(\lambda)\equiv\Omega=0$). Neutral stability curves for static instability are marked in Fig. 2(a) by closed solid lines. These static zones are independent from the delay time τ. In its turn, Hopf instability is absent at $\tau=0$ and appears above some threshold value of τ [10,12] within the same e_0 interval as the static instability. Boundaries of Hopf instability are marked by dots in Fig. 2(a) at $\tau=18$. Due to the transcendental structure, the algebraic equation obtained from Eq. (10) has several roots $\mathrm{Re}(\lambda_i)>0,\Omega_i\neq 0$, the number of which grows with increasing τ. As a consequence of this, we can seen in Fig. 2(a) where the secondary Hopf zones are dipped into the primary ones. Frequencies corresponding to the Hopf boundaries in Fig. 2(a) are plotted versus diffractional parameter θ in Fig. 2(b).

The appearance of new Hopf zones is illustrated more clearly in Fig. 3, where the Hopf frequencies Ω_i, the phase slippage created by delay $\Omega_i\tau$, as well as the lower and upper boundaries of instability domains versus the e_s axis are shown with increasing τ. One can see that a new zone appears with the increase of τ in $\Delta\tau\approx 9$. In Fig. 3(a) at small $\tau(\tau<20)$, two values of Ω_i for each abscissa value can be seen. They correspond to upper and lower zone boundaries of Fig. 3(c). For larger τ, Hopf frequencies are nearly constant in the limits of the zone. It should be noted that the data in Fig. 3 are obtained for fixed diffraction parameter $\theta=\theta_1$ as marked in Fig. 2. If we add the Hopf zones which occur at θ_2, we obtain two times more zones with the frequencies lying between that in Fig. 3. The curves in Figs. 3(a) and 3(b) confirm a general feature inherent in nonlinear system with delay [13,14]: The frequencies are inversely proportional to the delay time.

Let us return to Fig. 2(b), which is the key picture for understanding of interplay between diffraction and delay in our pattern-forming system. Vertical dashed lines denote critical values of θ at certain chosen incident light amplitude

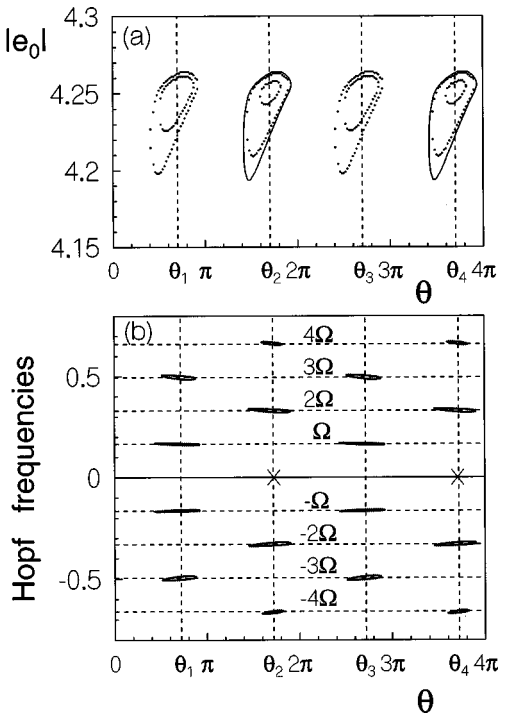

FIG. 2. (a) Neutral stability curves for $C=3.5$, $\delta=-2$, and $\tau=18$. Solid (dotted) curves limit domains of static (Hopf) instability. (b) Hopf frequencies on the boundaries shown in (a). Points of static instability are marked with $\times$.

($e_0=4.25$). Equidistant horizontal lines show average Hopf frequencies. Here, $\Omega=2\pi/T$ (where $T\approx 2\tau$) is a fundamental frequency. Note that T approach 2τ with increasing τ. Thus any excited mode is characterized by a ''knot'' (θ_i,Ω_i) of a lattice in Fig. 2(b). To proceed with discussion of Fig. 2, let us examine Eq. (10) more carefully. If delay time τ is enough large, Ω is small (cf. Fig. 3) and the right-hand side is inessential for determining marginal stability conditions.

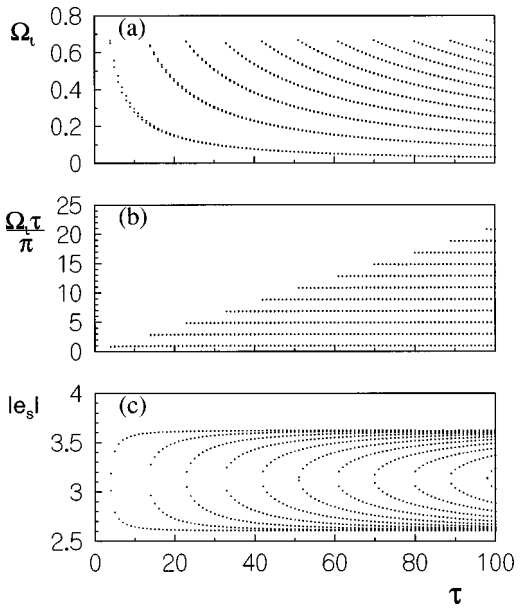

FIG. 3. Dependencies of (a) the Hopf frequencies Ω_i, (b) the phase slippage in the feedback loop $\Omega_i\tau$, and (c) the unstable e_s interval on the delay time τ.

In this case, the condition of the determinant of the matrix in the left-hand side being zero gives the instability threshold. One can see from the matrix that the delay parameter τ and the diffraction parameter θ enter the equation through the phase factor $e^{i\theta-i\Omega\tau}$. If at some θ static instability occurs, this instability takes place also at $\theta+2\pi n$, where n is integer. θ_2 and θ_4 in Fig. 2 show θ values for static instability. If we assume that the phase slippage $2\pi n$ is achieved on account of $\Omega\tau$, we obtain a family of Hopf instabilities with even frequencies,

$$\Omega_n=\frac{2\pi}{T}2n, \quad n=\pm 1,\pm 2,\ldots. \tag{11}$$

To obtain another family of the Hopf modes, we should make two shifts in π: one shift along a horizontal line in Fig. 2(b) (e.g., from θ_2 to θ_1) and another shift along a vertical line. Thus the frequencies of odd modes are

$$\Omega_n=\frac{2\pi}{T}(2n+1), \quad n=0,\pm 1,\pm 2,\ldots. \tag{12}$$

Having in mind that each θ zone implies an annulus of unstable wave vectors on the plane (k_x,k_y), we can find a variety of combinations satisfying conditions of three-wave mixing, (1) and (2). Note that the triadic Hopf-static patterns [10] (i.e., patterns created by two Hopf and one static modes) are particular cases of such mixing. There are only questions: (i) Is a quadratic coupling strong enough to support a resonant triad and (ii) will a Hopf triad survive in competition with other triadic patterns (e.g., ordinary hexagons)? Below we answer these questions by means of numerical simulations.

IV. RESULTS OF SIMULATIONS

We carried out numerical simulations by using an explicit scheme to integrate the Bloch equations and by using the fast Fourier transform to propagate an electrical field in free space between the film and the mirror. To take into account the delay effect, the data were stored in the time interval $[t,t-\tau]$. A spatial grid of 64×64 was commonly used (with 128×128 for checking). Periodic boundary conditions were assumed. The choice of the initial conditions was of important significance. Initial conditions corresponding to the ground state of the two-level system ($r=0,w=-1$) led to the triadic Hopf-static states described in Ref. [10]. To obtain stable resonant Hopf triads, we manipulated the Fourier image of the pattern in the feedback loop. (It should be noted that selection and control of patterns by manipulating their Fourier transform is natural for optical systems because of a property of a simple lens [25]). Namely, having a triadic Hopf-static pattern at our disposal we filtered static components from the 2D spatial Fourier spectrum and readdressed the Hopf mode from one $\mathbf{k}_\perp$ site to another, permitting the building of pure Hopf resonant constructions. Note that all structures demonstrated below are asymptotically stable patterns which correspond to solutions of the system when any filtering is omitted.

In Fig. 4, a motion of the Hopf pattern is illustrated for the incident field marked by the dashed line in Fig. 1(a) and for

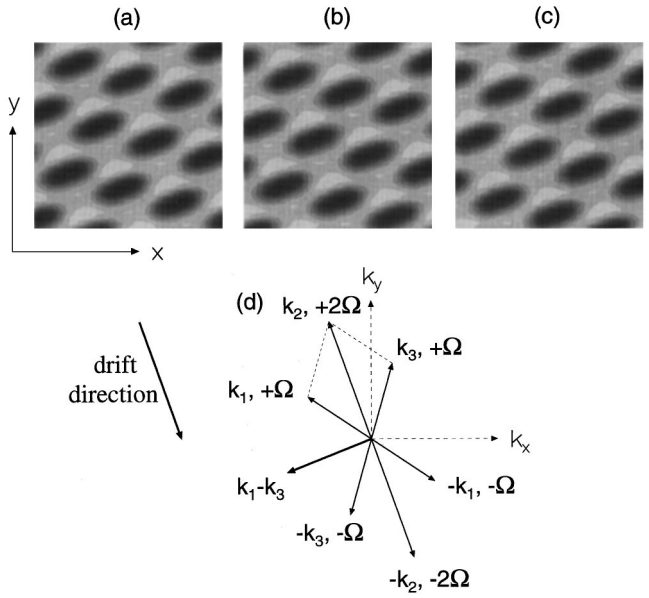

FIG. 4. (a)–(c) Snapshots of drifting triadic Hopf pattern obtained at three successive moments of time for the parameters of Fig. 2 and $|e_0|=4.25$. (d) illustrates instantaneous 2D Fourier spectrum.

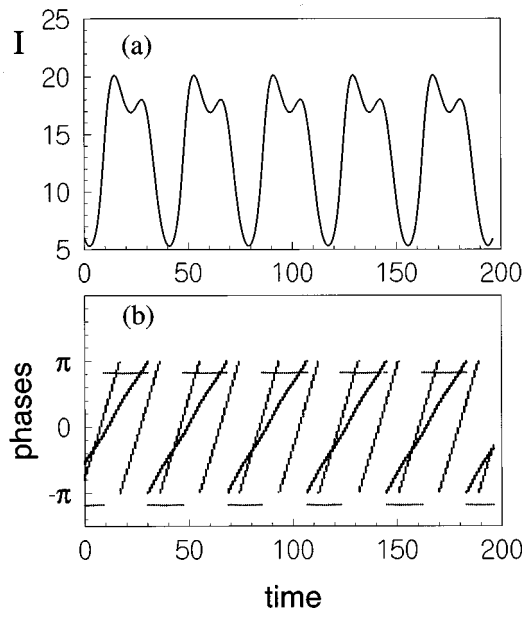

FIG. 5. Time evolution of (a) the local transmitted intensity and (b) the phase of the mode $(\mathbf{k}_1,+\Omega)$ in Fig. 4(d) (thin inclined curves), the phase of the mode $(\mathbf{k}_2,+2\Omega)$ (thick inclined curves), and the sum of the resonant Hopf modes (thin horizontal curves).

$\tau=18$. The patterns in Figs. 4(a)–4(c) are snapshots of light intensity transmitted through the film. (Here and in the pictures below, only one-quarter of the whole simulated area is shown.) The time interval between the subsequent snapshots is $\tau/2$ that corresponds to approximately a quarter of the full period. Wave vectors of three Hopf modes composing a pattern are shown in the (k_x,k_y) plane in Fig. 4(d). The modes with the wave vectors $\mathbf{k}_1$ and $\mathbf{k}_3$ oscillating with the frequency Ω belong to the θ_1 band of Fig. 2, whereas the mode $(\mathbf{k}_2,2\Omega)$ is excited due to the instability θ_2 band. One can see that spatiotemporal phase matching is fulfilled.

Let us discuss a pattern evolution by writing down an explicit expression for the transmitted light intensity

$$I=I_{dc}+\frac{1}{2}H_1e^{i\mathbf{k}_1\mathbf{r}_\perp+i\Omega t}+\frac{1}{2}H_2e^{i\mathbf{k}_2\mathbf{r}_\perp+i2\Omega t}+\frac{1}{2}H_3e^{i\mathbf{k}_3\mathbf{r}_\perp+i\Omega t}+\text{c.c.}, \tag{13}$$

where H_i are complex amplitudes of the Hopf modes. Assuming that $H_1=H_3$, we can reduce Eq. (13) to

$$I=I_{dc}+2H_1\cos\left(\frac{\mathbf{k}_1-\mathbf{k}_3}{2}\mathbf{r}_\perp\right)\cos\left(\frac{1}{2}(\mathbf{k}_2\mathbf{r}_\perp+2\Omega t)\right)+H_2\cos(\mathbf{k}_2\mathbf{r}_\perp+2\Omega t). \tag{14}$$

As it follows from Eq. (14), the pattern performs motion with a velocity $2\Omega/|\mathbf{k}_2|$ in the direction $-\mathbf{k}_2$ (see Fig. 4). Obviously, because of a symmetry of the system, any other resonant triad obtained from the one drawn in Fig. 4(d) by rotation around the origin is also possible. It means that direction of motion is determined by the initial conditions.

Figure 5 gives further numerical information about pattern evolution. The curve in Fig. 5(a) presents oscillations of the local transmitted intensity. Figure 5(b) shows phases of modes running with velocities Ω (thick line) and 2Ω (thin line). Of special importance is the sum of the phases of the modes $(\mathbf{k}_1,+\Omega)$, $(\mathbf{k}_3,+\Omega)$, and $(-\mathbf{k}_2,-2\Omega)$ which form the resonant triad. This characteristic is given in Fig. 5 by the horizontal lines at the levels of nearly 0.8π and -1.2π. Analogously with the cases of the static hexagons [26] and of the triadic Hopf-static patterns [10] we could refer to our structure as negative or π triadic Hopf structures if the sum would be exactly $\pm\pi$ (i.e., the dark spots on the light background are an attribute of negative triadic structures). However, our situation appears to be a little more sophisticated. This is connected with a motion of the pattern. As can be seen from Fig. 5(a) as well as from Figs. 4(a)–4(c), a drift of the pattern leads to the feature that distributions of the intensity before the dark spot and behind it are not equal. In other words, a drifting dark spot leaves something like a short ''tail.'' Thus we can refer to our structure as a negative triadic Hopf structure distorted by a motion.

Another kind of triadic Hopf structure obtained for the same parameters is presented in Fig. 6. Similar to the previous picture, three snapshots are shown in time interval $\tau/2$. Here, the distinction from the previous case is that all three wave vectors $\mathbf{k}_i$ [see Fig. 6(d)] have different lengths (i.e., three Hopf modes belong to different θ bands of Fig. 2). Because of this, the pattern has rhomboidal symmetry. As in Fig. 4, the pattern in Fig. 6 performs a drifting motion in the direction perpendicular to $\mathbf{k}_1-\mathbf{k}_3$. Again, the sum of the phases of three modes composing the resonant triad is close but not exactly $\pm\pi$.

Hopf modes can also build the structures of hexagonal symmetry. For this, three wave vectors must be of equal length, i.e., they should belong to the same instability θ band in Fig. 2. However, not every θ band is suitable for the generation of drifting hexagon patterns. Let us note that the composition of two Hopf modes with odd frequencies

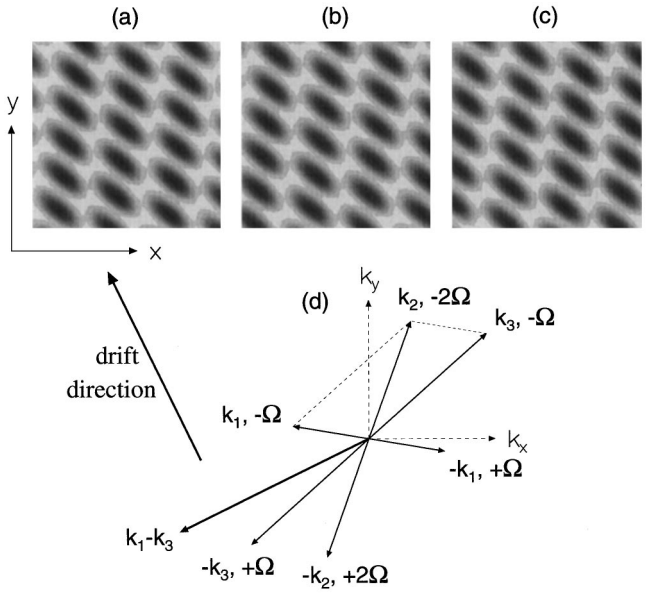

FIG. 6. Triadic Hopf pattern composed of the modes with three different k_i and obtained at the same parameters as the pattern in Fig. 4. (a)–(c) are three snapshots. (d) illustrates instantaneous 2D Fourier spectrum.

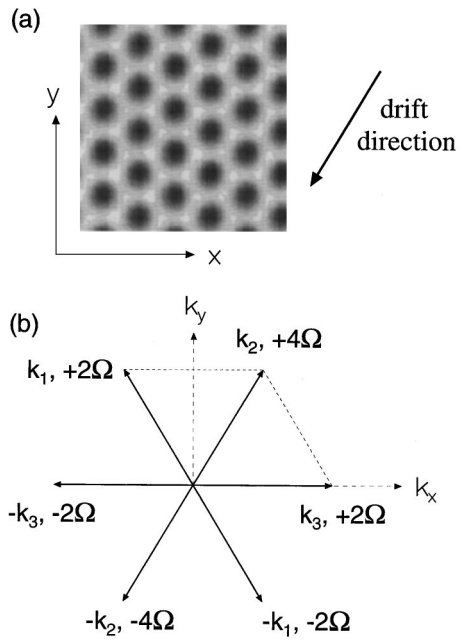

FIG. 7. (a) Triadic Hopf structure in the form of drifting hexagons and (b) its Fourier image.

$(2n+1)\Omega$ will give the mode with even frequency. Therefore, for creation of Hopf hexagons, the θ_i zones with even subscipts i should be used. In Fig. 7(a), a snapshot of drifting hexagon structure is shown. Velocity and direction of motion are evident from consideration of Fig. 7(b), i.e., the pattern runs in the direction of the vector $-\mathbf{k}_2$ with the velocity $2\Omega/|\mathbf{k}_2|$.

All the patterns presented above are obtained for the same parameters, i.e., the system demonstrates multistability. Switching from one pattern to another can be achieved by manipulating the Fourier image. We have not had an aim in this paper to find all possible states of the system, but it is natural to suppose that the number of possible stable triadic Hopf patterns grows with increasing τ.

The circumstance that we have observed patterns similar to π structures (i.e., dark spots on the light background) is explained by the fact that our simulations have been carried out for the set of parameters ($e_0=4.25$) close to the upper instability boundary [see Fig. 2(a)]. This matches the proof in Ref. [10] that negative (positive) Hopf-static structures should be near the upper (lower) instability boundary, i.e., the quadratic coupling changes its sign from upper to lower boundary. Indeed, at $e_0=4.22$ we have observed positive triadic Hopf patterns of rhombic symmetry (like the one in Fig. 4 with the only difference being inverse contrast) with the sum of the phases of resonant modes close to zero. However, this pattern was not asymptotically stable and after transient time changed into positive static hexagons.

V. CONCLUSION

We have shown that an optical pattern-forming system demonstrates a dissipative structure which is a result of mixing of three Hopf modes. In our concrete case, the Hopf instability is determined by the delay effect. In general, time delay is important as far as it introduces infinite degrees of freedom into dynamical system [14,15]. One might deduce that the resonant Hopf triad may be observed in a nonlinear pattern-forming system without delay when there are enough internal degrees of freedom to provide multiple Hopf bifurcations.

We have not taken into account transverse diffusion in our model. Evidently, the diffusion processes will suppress the instability θ_i zones with large index i so that large-scale structures should be preferred in real experiments.

Recently, the modifications of the single-feedback-mirror scheme have been considered which imply either a tilted mirror [27,28] or a nonlocal interaction introduced by a translation [29]. Both these modifications cause a static pattern to run along a prescribed direction. In other words, the static instability turns into the Hopf one, and thus there appear favorable conditions for emergence of triadic Hopf patterns.

[1] V. N. Tsytovich, *Nonlinear Effects in Plasma* (Plenum Press, New York, 1970).

[2] B. B. Kadomtsev, *Collective Phenomena in Plasma* (Nauka, Moscow, 1976) (in Russian).

[3] O. M. Phillips, *The Dynamics of the Upper Ocean*, 2nd ed. (Cambridge University Press, Cambridge, England, 1977).

[4] A. D. D. Craik, *Wave Interactions and Fluids Flows* (Cambridge University Press, Cambridge, England, 1985).

[5] V. S. L'vov, *Wave Turbulence Under Parametric Excitation* (Springer, Berlin, 1994).

[6] F.-J. Elmer, Phys. Rev. B **53**, 14 323 (1996).
[7] Y. R. Shen, *The Principles of Nonlinear Optics* (Wiley, New York, 1984).
[8] M. C. Cross and P. C. Hohenberg, Rev. Mod. Phys. **65**, 851 (1993).
[9] D. Lima, A. De Wit, G. Dewel, and P. Borckmans, Phys. Rev. E **53**, R1305 (1996).
[10] Yu. A. Logvin, B. A. Samson, A. A. Afanas'ev, A. M. Samson, and N. A. Loiko, Phys. Rev. E **54**, R4548 (1996).
[11] A. De Wit, D. Lima, G. Dewel, and P. Borckmans, Phys. Rev. E **54**, 261 (1996).
[12] N. A. Loiko, Yu. A. Logvin, and A. M. Samson, Opt. Commun. **124**, 383 (1996).
[13] K. Ikeda, K. Kondo, and O. Akimoto, Phys. Rev. Lett. **49**, 1467 (1982).
[14] K. Ikeda and K. Matsumoto, Physica D **29**, 223 (1987).
[15] E. V. Grigorieva, S. A. Kashchenko, N. A. Loiko, and A. M. Samson, Physica D **59**, 297 (1992).
[16] W. J. Firth, J. Mod. Opt. **37**, 151 (1990); G. D'Alessandro and W. J. Firth, Phys. Rev. A **46**, 537 (1992).
[17] D. Leduc, M. Le Berre, E. Ressayre, and A. Tallet, Phys. Rev. A **53**, 1072 (1996); M. Le Berre, D. Leduc, E. Ressayre, and A. Tallet, *ibid.* **54**, 3428 (1996).
[18] E. V. Degtiarev and M. A. Vorontsov, J. Mod. Opt. **43**, 93 (1996).
[19] E. Pampaloni, S. Residori, S. Soria, and F. T. Arecchi, Phys. Rev. Lett. **78**, 1042 (1997).
[20] K. Patorski, *The Self-imaging Phenomenon and Its Applications*, Progress in Optics. Vol. XXVII, edited by E. Wolf (North-Holland, Amsterdam, 1989), p. 3.
[21] M. J. Benedikt and E. D. Trifonov, Phys. Rev. A **38**, 2854 (1988).
[22] Yu. A. Logvin and A. M. Samson, Opt. Commun. **96**, 107 (1993).
[23] L. Allen and J. H. Eberly, *Optical Resonance and Two-Level Atoms* (Wiley, New York, 1975).
[24] A. A. Afanas'ev, Yu. A. Logvin, A. M. Samson, and B. A. Samson, Opt. Commun. **115**, 559 (1995).
[25] R. Martin, A. J. Scroggie, G.-L. Oppo, and W. J. Firth, Phys. Rev. Lett. **77**, 4007 (1996).
[26] S. Ciliberto, P. Coullet, J. Lega, E. Pampaloni, and C. Perez-Garcia, Phys. Rev. Lett. **65**, 2370 (1990).
[27] A. Petrossian, L. Dambly, and G. Grynberg, Europhys. Lett. **29**, 209 (1995).
[28] T. Ackemann, J. Seipenbusch, B. Berge, B. Schäpers, Yu.A. Logvin, and W. Lange, Quantum Electronics and Laser Science Conference, Baltimore, Maryland, May 1997, OSA Techn. Digest Series, Vol. 12, pp. 111–112.
[29] P. L. Ramazza, P. Bigazzi, E. Pampaloni, S. Residori, and F. T. Arecchi, Phys. Rev. E **52**, 5524 (1995); P. L. Ramazza, S. Boccaletti, A. Giaguinta, E. Pampaloni, S. Soria, and F. T. Arecchi, Phys. Rev. A **54**, 3472 (1996).